SAND REPORT

SAND2005-7134
Unlimited Release
Printed December 2005

New Self-Assembled Nanocrystal Micelles For Biolabels and Biosensors

Hongyou Fan, Erik W. Leve, Chessa Scullin, John Gabaldon, David Tallant, Michael C. Wilson, C. Jeffrey Brinker

Prepared by
Sandia National Laboratories
Albuquerque, New Mexico 87185 and Livermore, California 94550

Sandia is a multiprogram laboratory operated by Sandia Corporation, a Lockheed Martin Company, for the United States Department of Energy under Contract DE-AC04-94AL85000.

Issued by Sandia National Laboratories, operated for the United States Department of Energy by Sandia Corporation.

Available to DOE and DOE contractors from
U.S. Department of Energy
Office of Scientific and Technical Information
P.O. Box 62
Oak Ridge, TN 37831

Telephone: (865)576-8401
Facsimile: (865)576-5728
E-Mail: reports@adonis.osti.gov
Online ordering: http://www.doe.gov/bridge

Available to the public from
U.S. Department of Commerce
National Technical Information Service
5285 Port Royal Rd
Springfield, VA 22161

Telephone: (800)553-6847
Facsimile: (703)605-6900
E-Mail: orders@ntis.fedworld.gov
Online order: http://www.ntis.gov/ordering.htm

SAND2005-7134
Unlimited Release
Printed December 2005

New Self-Assembled Nanocrystal Micelles for Biolabels and Biosensors

Hongyou Fan[a,b,*], Erik W Leve[b], Chessa Scullin[c], JohnP. Gabaldon[b], David R. Tallant[a], Michael Wilson[c], and C. Jeffery Brinker[b,d]

[a]Chemical Synthesis and Nanomaterials Department, Sandia National Laboratory, P.O. 5800, Albuquerque, NM 87185-1349

[b]Chemical and Nuclear Engineering Department, Center for Micro-Engineered Materials, University of New Mexico, Albuquerque, NM 87106

[c]Department of Neuroscience,
School of Medicine,
University of New Mexico,
Albuquerque, NM

[d]Self-Assembled Materials Department

Sandia National Laboratories, P.O. 5800, Albuquerque, NM 87185-1349

Abstract

The ability of semiconductor nanocrystals (NCs) to display multiple (size-specific) colors simultaneously during a single, long term excitation holds great promise for their use in fluorescent bio-imaging. The main challenges of using nanocrystals as biolabels are achieving biocompatibility, low non-specific adsorption, and no aggregation. In addition, functional groups that can be used to further couple and conjugate with biospecies (proteins, DNAs, antibodies, etc.) are required. In this project, we invented a new route to the synthesis of water-soluble and biocompatible NCs. Our approach is to encapsulate as-synthesized, monosized, hydrophobic NCs within the hydrophobic cores of micelles composed of a mixture of surfactants and phospholipids containing head groups functionalized with polyethylene glycol (-PEG), -COOH, and $-NH_2$ groups. PEG provided biocompatibility and the other groups were used for further biofunctionalization. The resulting water-soluble metal and semiconductor NC-micelles preserve the optical properties of the original hydrophobic NCs. Semiconductor NCs emit the same color; they exhibit equal photoluminescence (PL) intensity under long-time laser irradiation (one week); and they exhibit the same PL lifetime (30-ns). The results from transmission electron microscopy and confocal fluorescent imaging indicate that water-soluble semiconductor NC-micelles are biocompatible and exhibit no aggregation in cells. We have extended the surfactant/lipid encapsulation techniques to synthesize water-soluble magnetic NC-micelles. Transmission electron microscopy results suggest that water-soluble magnetic NC-micelles exhibit no aggregation. The resulting NC-micelles preserve the magnetic properties of the original hydrophobic magnetic NCs. Viability studies conducted using yeast cells suggest that the magnetic nanocrystal-micelles are biocompatible. We have demonstrated, for the first time, that using external oscillating magnetic fields to manipulate the magnetic micelles, we can kill live cells, presenting a new magnetodynamic therapy without side effects.

* Author to whom correspondence should be addressed (hfan@sandia.gov)

Acknowledgements

We would like to thank Drs. John Guzowski and Teiko Miyashita for training and help with fluorescent microscopy. This work was partially supported by the U.S. Department of Energy (DOE) Basic Energy Sciences Program, Sandia National Laboratory's Laboratory Directed R&D program, the Air Force Office of Scientific Research, NSF/UNM Science and Learning Center (SLC) Catalyst/Planning Grant, and Center for Integrated Nanotechnologies (CINT). TEM studies were performed in the Department of Earth and Planetary at University of New Mexico. Sandia is a multiprogram laboratory operated by Sandia Corporation, a Lockheed Martin Company, for the United States Department of Energy's National Nuclear Security Administration under Contract DE-AC04-94AL85000.

Contents

Scheme and Figures

Introduction

Semiconductor quantum dots (QDs) with superior optical properties are a promising alternative to organic dyes for fluorescence-based bio-applications. The potential benefits and use of conjugated QD probes to monitor cellular functions has prompted extensive efforts to develop methods to synthesize water-soluble and biocompatible QDs that can be widely used for fluorescent-based bio-imaging[1-7]. In general, the key to developing QDs as a tool in biological systems is to achieve water-solubility, biocompatibility and photo-stability. Further it is important to provide flexible QD surface chemistry/functionality that will enable efficient coupling of these fluorescent inorganic probes to reagents capable of targeting and/or sensing ongoing biological processes. To date, most of the work has focused on the synthesis and self-assembly of nanocrystals that are stabilized with alkane ligands ($CH_3(CH_2)_nR$, R=SH, NH_2, PO, etc)[8-10]. Such NCs can be made at fairly high quality (narrow size distribution, preferred shapes such as rod, cube, etc, and large production). These NCs are hydrophobic, and their self-assembly is limited to organic solvents. However, there are many applications requiring hydrophilic or aqueous environments, such as biolabeling and SERS-based NC films or arrays for biosensing[11-13]. In addition, water-soluble NCs and their ordered arrays/films provide great opportunity for further integration into inorganic ceramic frameworks that offer the chemical and mechanical robustness needed for enhanced device functionality[14, 15]. In this project, we developed a facile method to prepare NC-micelles in aqueous media. The method is to incorporate monosized, hydrophobic NCs into the hydrophobic interiors of surfactant micelles[16-19]. The uniform NC size and self-assembled monolayer-like nature of its surface result in the formation of monosized gold NC-micelles composed of a gold NC core and a hybrid bilayer shell with precisely defined primary and secondary layer thicknesses (see scheme 1). By using phospholipids, we extended this technique to the synthesis of water-soluble, biocompatible semiconductor QD-micelles. This synthetic approach avoids complicated multi-step procedures and promises to add to the versatility of QD-based probes for investigating intracellular transport and other cellular signaling pathways in living cells.

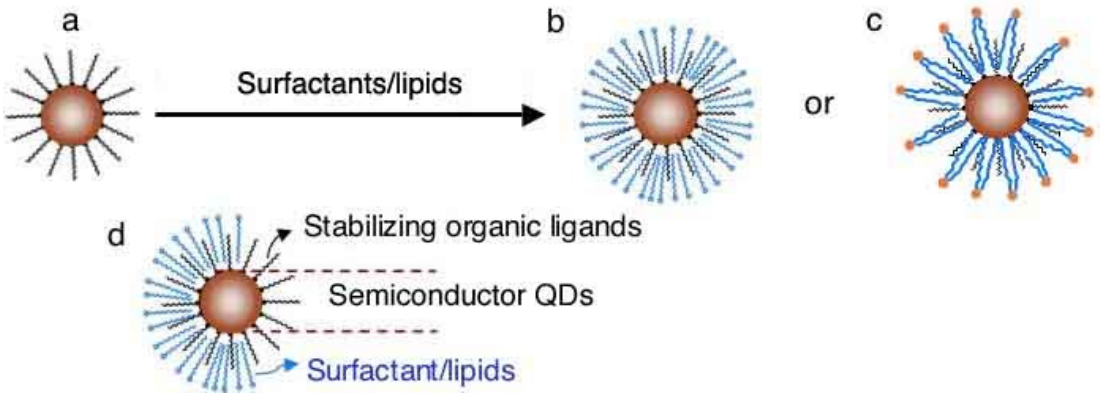

Scheme 1. Formation of water-soluble QD-micelles through incorporation in surfactant or phospholipid micelles. a. An Oleilic acid (OA)-stabilized CdSe/CdS QD; b and c. OA-stabilized CdSe/CdS QDs are encapsulated inside surfactant/lipid micelles using an oil-in-water microemulsion technique where evaporation of oil drives interfacially mediated QD transfer into water-soluble micelles; d. Thermodynamically defined interdigitated "bilayer" structure stabilized QDs in water.

Results and Discussion

An alkane chain stabilized NC can be envisioned as a giant hydrophobic "molecule" that can be individually encapsulated into the hydrophobic core of a surfactant micelle in water. During the formation of NC-micelles, surfactants serve as active agents to reduce repulsion between hydrophobic NCs and water. The thermodynamically defined interdigitated "bilayer" structure between the primary layer and secondary layer contributes extensive energy (van der Waals interactions) to stabilize NC-micelles in water[20-22]. We conducted differential scanning calorimetry (DSC) experiments on the dried powder samples of gold NC-micelles that were prepared using dodanethiol-stabilized gold NC and surfactants with different alkane chain lengths (C12TAB, C14TAB, and C16TAB). We observed that each sample exhibited an endothermic peak. These peaks appear at ~11.5˚C for the NC-C12TAB sample, ~47˚C for the NC-C14TAB sample, and ~72˚C for the NC-C16TAB sample; the temperature of the peak maxima increases with increasing alkane chain length. This suggests that longer alkane chains contribute more extensive van der Waals interactions. The

advantage of the surfactant encapsulation technique is that the interdigitated bilayer involves no chemical reactions, and therefore will not change the physical properties (optical, aggregation, electronic, etc) of the original NCs.

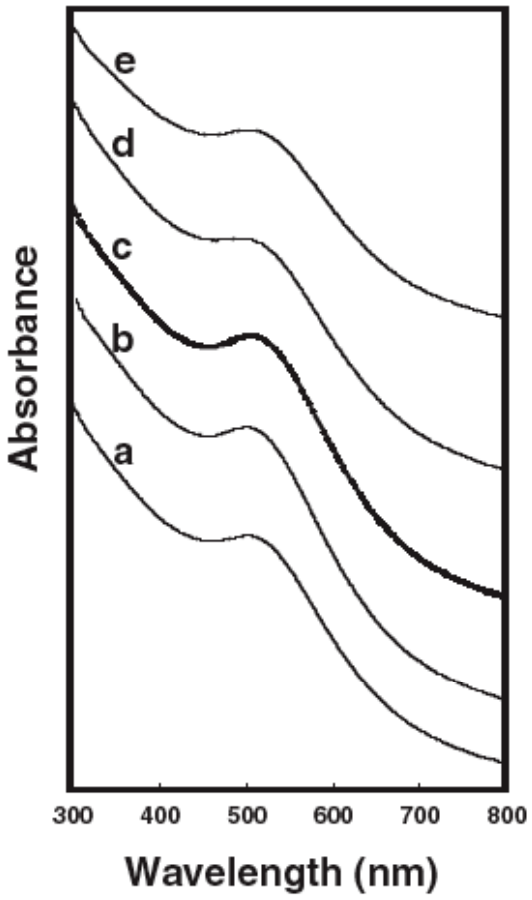

Figure 1. UV-visible spectra of (a) gold NCs in chloroform; (b) gold NC-micelles prepared using cationic surfactant: $CH_3(CH_2)_{15}N^+(CH_3)_3Br^-$ in water; (c). Gold NC-micelle prepared by using anionic surfactant: $CH_3(CH_2)_{11}SO_3^-\ Na^+$, SDS; (d). Gold NC-micelles prepared by using nonionic surfactant: $CH_3(CH_2)_{15}$-$(OCH_2CH_2)_{10}$-OH, Brij58 in water; (e). Gold NC-micelles prepared using 1,2-dioctanoyl-*sn*glycero-3-phosphocholine in water.

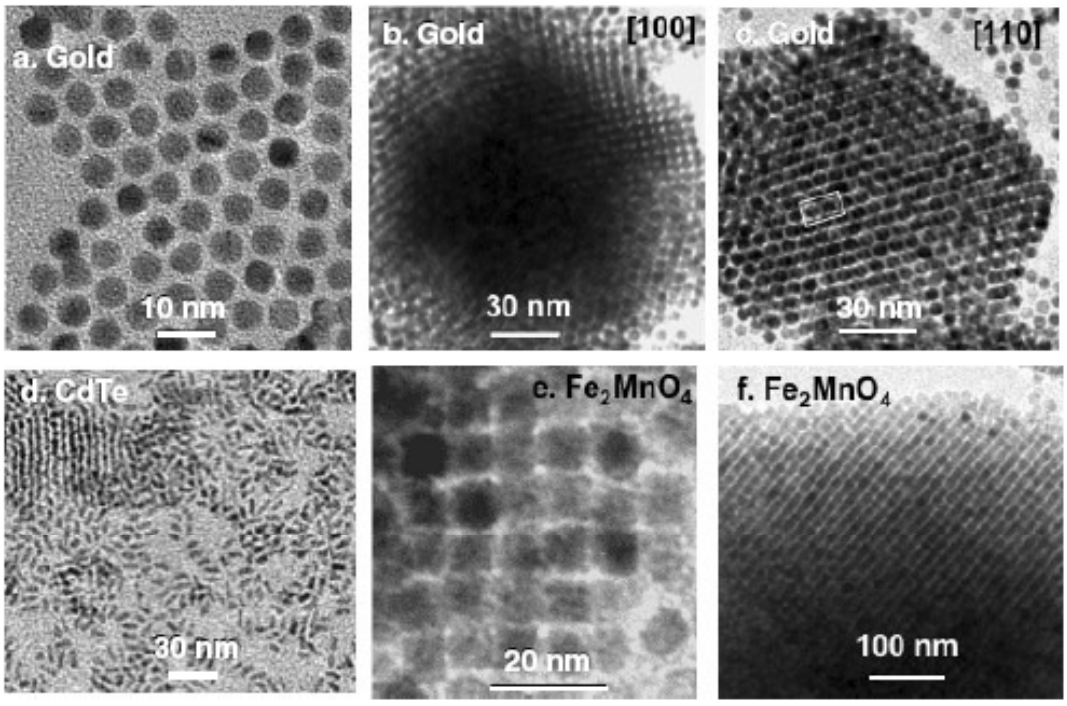

Figure 2. Representative transmission electron micrographs (TEM) of ordered NC-micelle superlattices. (a). 2-D gold NC-micelle arrays with hexagonal close packing; (b). [100] orientation of 3-D gold NC-micelle superlattice arrays; (c). [110] orientation of 3-D gold NC-micelle superlattice arrays; (d). Ordered CdTe nanorod-micelle arrays; (e). 2-D Fe_2MnO_4 nanocube-micelle arrays; (f). [100] orientation of 3-D ordered Fe_2MnO_4 nanocube-micelle arrays.

Formation and stability of monodisperse gold NC-micelles have been confirmed using UV-visible spectroscopy (Fig. 1) and transmission electron microscopy (TEM, Fig. 2). Figure 1a shows the spectra of DT-stabilized gold NCs in chloroform. The absorbance at ~520-nm corresponds to the gold surface plasmon resonance band. Figure 1b shows the spectra of gold NC-micelles in water prepared using cationic surfactant CTAB. By comparison of Figure 1a and 1b, we observe no difference in the positions and peak widths of the plasmon resonance band of the DT-stabilized gold NCs in chloroform and those of the corresponding water-soluble NC-micelles. This suggests that gold NC-micelles remain monodisperse in water without aggregation, which is further confirmed by TEM (see below). Similar results in Figure 1c through 1e suggest that anionic surfactants, non-ionic surfactants, and phospholipids can all form NC-micelles as well as cationic surfactants. Advantageously,

this allows facile control of NC-micelle surface charge and functionality via functional groups such as polyethylene glycol (PEG), hydroxyl (-OH), etc.

Due to the monodipsersity of resulting NC-micelles, they can self-assemble into 2- and 3-D superlattice films through evaporation of drops of NC-micelle water solution onto solid substrates such as Si wafers, glass, TEM grids. Figure 2a shows a representative TEM image of the hexagonal close packing (*hcp)* 2-D superlattice resulting from drying of a gold NC-micelle solution on an amorphous carbon-coated copper grid. The mean interparticle spacing was estimated to be ~3-nm by direct measurement of individual spacing within well-ordered domains. The formation of ordered *hcp* 2-D arrays, as is expected for individual, monosized NCs, further confirms that gold NC-micelles remain monodisperse in water without aggregation. In addition to spherical NCs, we extended the concept to stabilize and self-assemble NCs with other shapes such as rods and cubes. CdTe nanorods were prepared according to Peng *et al*[23] using trioctylphosphine oxide as a stabilizing agent. The encapsulation was conducted using CTAB. The TEM image (Figure 2d) revealed that surfactant "bilayer" stabilized CdTe nanorods formed uniform arrays. Fe_2MnO_4 nanocubes were prepared according to Zeng *et al*[17] using oleylamine as a stabilizing agent. Formation of Fe_2MnO_4 nanocube-micelles was conducted using CTAB. The TEM image (Figure 2e) shows that the Fe_2MnO_4 NC-micelles self-organize into ordered arrays with cubic symmetry. We have extended the surfactant/lipid encapsulation techniques to synthesize water-soluble and biocompatible magnetic NC-micelles. Transmission electron microscopy results suggest that these magnetic NC-micelles exhibit no aggregation. The resulting NC-micelles preserve the magnetic properties of the original hydrophobic magnetic NCs. Viability studies conducted using yeast cells suggest that the magnetic nanocrystal-micelles are biocompatible. We have demonstrated, for the first time, that using external oscillating magnetic fields to manipulate the magnetic micelles, we can kill live cells, presenting a new magnetodynamic therapy without side effects.

We then used the surfactant encapsulation method to synthesize water-soluble and biocompatible spherical semiconductor NC-micelles. Monodisperse CdSe and CdSe/CdS

core/shell QDs were synthesized according to previous methods using trioctylphosphine

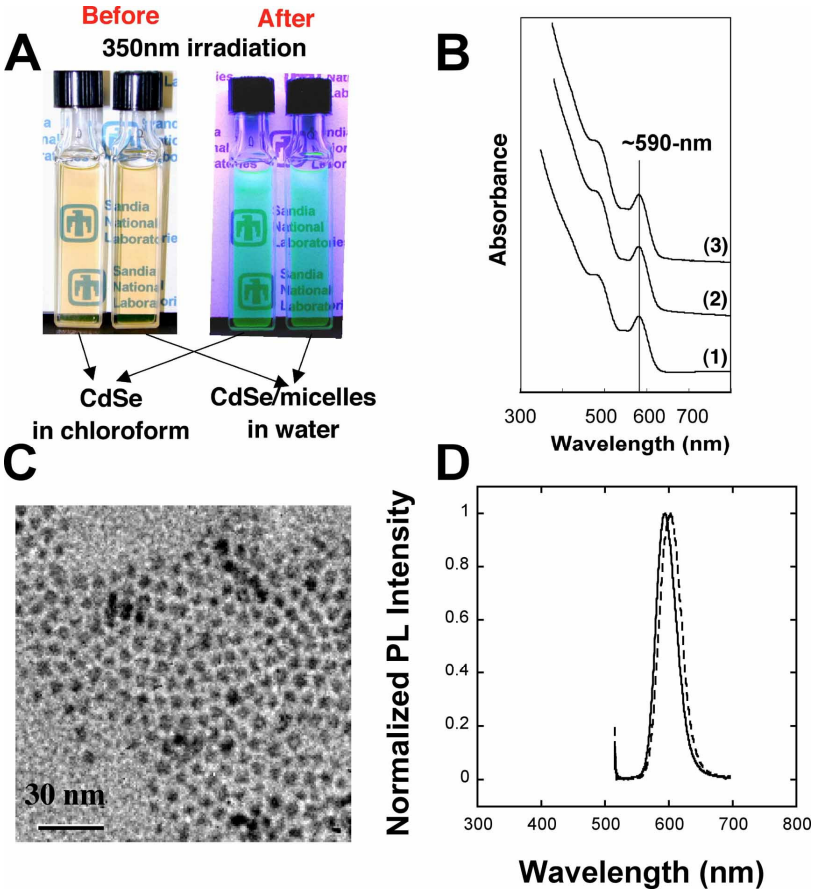

(TO) and

Figure 3. A. An optical micrograph of CdSe QDs in chloroform and CdSe-micelles in water prepared using cetyltrimethylammonium bromide and imaged under room light and 350-nm UV light. B. UV-vis spectra of (1) CdSe/CdS in hexane, (2) CdSe/CdS-micelles prepared in phosphate buffer solution by using 1,2-Dioctanoyl-*sn*-Glycero-3-Phosphocholine (C8-lipid) and hexadecylamine (HDA), and (3) 1,2-Distearoyl-*sn*-Glycero-3-Phosphoethanolamine-N-Amino (Polyethylene Glycol) (aPEG) and dipalmitoyl phosphatidylcholine (DPPC). C. TEM image of CdSe/CdS-micelles deposited on TEM grid from a drop of CdSe/CdS-micelle water solution. D. Photoluminescence spectra of CdSe/CdS in toluene (solid line) and C8-lipid encapsulated CdSe/CdS-micelles in water (dashed line).

oleylamine (OA) as stabilizing agents[23]. In a typical QD-micelle synthesis procedure, a concentrated suspension of QDs in chloroform is added to an aqueous solution containing a mixture of surfactants or phospholipids with different functional head groups such as

ethylene glycol (-PEG) and amine (-NH_2). PEG is used to improve biocompatibility and amine groups provide sites for bioconjugation. Addition of the QD chloroform suspension into the surfactant/lipid aqueous solution under vigorous stirring results in the formation of an oil-in-water microemulsion. Evaporation of chloroform during heating (40-80˚C, ~10 minutes) transfers the QDs into the aqueous phase by an interfacial process driven by the hydrophobic van der Waals interactions between the primary alkane of the stabilizing ligand and the secondary alkane of the surfactant, resulting in thermodynamically defined interdigitated bilayer structures (Scheme 1d). Based on evaluation of water-solubility and stability using ultraviolet-visible spectroscopy (UV-vis), transmission electron micrograph (TEM), and fluorescent spectra, optimized lipids were those with at least 6-8 carbons in their hydrophobic alkane chains.

QD-micelle solutions exhibited the same visible and emission colors as hydrophobic QDs, as shown in the optical micrograph (Fig. 3A). The formation of individual CdSe/CdS QD-micelles was further charaterized by UV-vis spectroscopy shown in Fig. 3B. We observed no difference in the position or width of the absorbance bands at ~480-nm and ~590-nm from hydrophobic QDs and QD-micelles, which suggests that QD-micelles maintain their optical properties in water. Formation of ordered hexagonal close packing shown in TEM (Fig. 3C), as expected for individual monosized QDs, further confirmed the monodispersity of QD-micelles. Photoluminescence (PL) spectra of OA-stabilized hydrophobic QD and QD-micelles prepared using 1,2-Dioctanoyl-*sn*-Glycero-3-Phosphocholine (C8-lipids) are shown in Fig. 3D. PL of QD-micelles exhibited no obvious shift in emission wavelength. Studies of photo-stability of these water-soluble NC-micelles under long-time laser irradiation showed that these QD-micelles exhibited no loss of PL intensity in water (Fig. 4A inset). The stability of QD-micelles in a cellular aqueous environment was confirmed by incubation with rat hippocampal neurons (see below).

The PL persistence (lifetime) from OA-stabilized CdSe/CdS in toluene, CdSe/CdS-micelle water solutions, and Rhodamine B (RB) in ethanol were measured and calculated according to Donega *et al* and are shown in Fig. 4A. The persistence was measured during

pulsed, 450-nm excitation by monitoring emission at the peak of the PL profile.

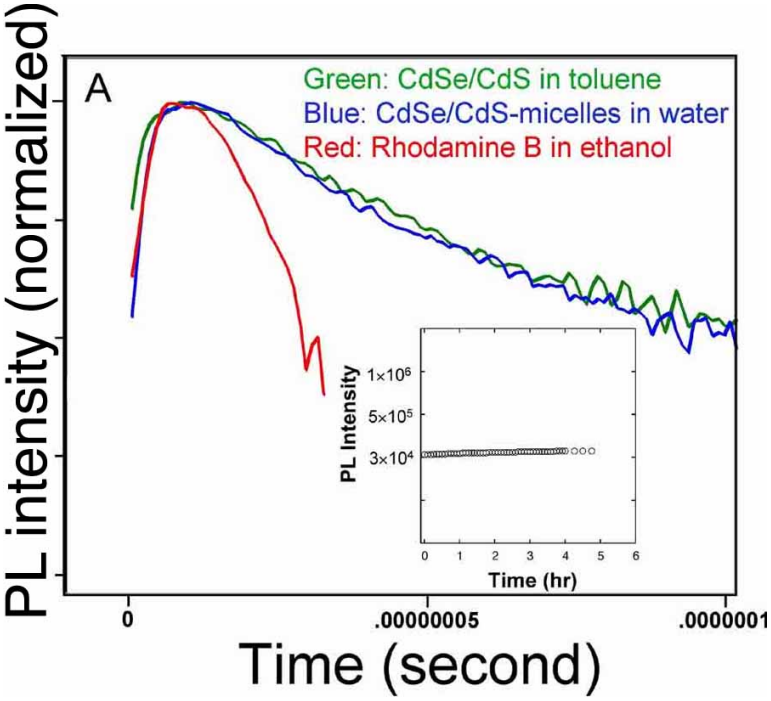

Figure 4. A. Persistence curves from CdSe/CdSe in toluene, RB in ethanol, and CdSe/CdS-micelles in water solution prepared by using C8-lipid. Inset. PL intensity CdSe/CdS-micelles in water solution vs laser irradiation time.

The RB persistence is only slightly longer than the instrumental bandwidth. The $\log_e$ plots of the persistence curves from the CdSe QDs in toluene and H_2O/C8-lipid solutions were similar and nearly linear, with a (1/e) relaxation constant of ~30 nanoseconds, which was much longer than the lifetime of RB (~5 nanoseconds).

The advantage of our method to provide water-soluble QD-micelles is its capability to utilize a wide variety of surfactants/lipids with different functionally-terminated groups, which can be used to improve biocompatibility and to enable bioconjugation. The encapsulation is accomplished in a single, rapid (10-minute) step of solvent evaporation. In our method, the stabilization of hydrophobic QDs in water relies on the thermodynamically favorable interdigitation of surfactants and QD stabilizing ligands formed after solvent evaporation, enabling rapid efficient transfer of the QDs into the aqueous phase. The QD-micelles preserve the optical properties of the original source QDs, such as PL intensity and lifetime etc., as the encapsulation process involves no chemical substitution reactions. In

contrast, in other methods, such as the ligand exchange method, chemical substitution occurs at the QD interface. This usually results in QD aggregation and changes in QD physical properties. Additionally, our method can effectively prevent QD-micelles from aggregation due to the interdigitated "bilayer."

To evaluate the biocompatibility of CdSe/CdS QD-micelles we performed an initial study to examine their uptake in cultured rat hippocampal neurons. While the route through which QDs are taken up by cells has yet to be resolved fully, they do appear to accumulate in intracellular vesicular compartments in several cell types suggesting uptake may be mediated, at least in part, though endocytosis. Because synaptic vesicle recycling is tightly coupled to neurotransmitter release, endocytosis can be manipulated by depolarization of the plasma membrane to excite neurons, evoking exocytosis for neurotransmitter release followed by endocytotic retrieval of synaptic vesicle membrane from nerve terminals. As shown in Figure 5A, QD-micelles (emission 592 nm, red) accumulate in neurons, distinguished by immmunohistochemical counterstain for NeuN (green), after exposure for 16 hours in basal serum-free growth media. A three-dimensional reconstruction of confocal images confirmed the intracellular localization of QD fluorescence after long-term exposure (see supplemental materials, movie 1). The observation that QDs retain their fluorescence character after a fairly long incubation suggests that QDs can accumulate without aggregation and a general compatibility of the micelle coating within a cellular environment.

In order to obtain a more detailed view of QD uptake, we used pulse-chase labeling to expose hippocampal cultures to QD-micelles during membrane depolarization (induced by addition of 55 mM KCl) to trigger neurotransmitter release and coupled exo/endocytosis, followed by a return to basal media. After a 10 min exposure to QDs during depolarization, robust QD fluorescence was detected by confocal microscopy in wide-spread, yet clustered pattern surrounding NeuN-positive neurons Figure 5, panel B), consistent with a diffuse, punctate localization and uptake in neuronal processes and synapses. Interestingly, following exchange for basal media without QDs, there was an apparent time-dependent increase in the perinuclear accumulation of QD fluorescence accompanied by a decrease in the more wide-spread distribution seen immediately after KCl depolarization (Figure 5, Panels C, D). By 5 hours, the majority of QD fluorescence

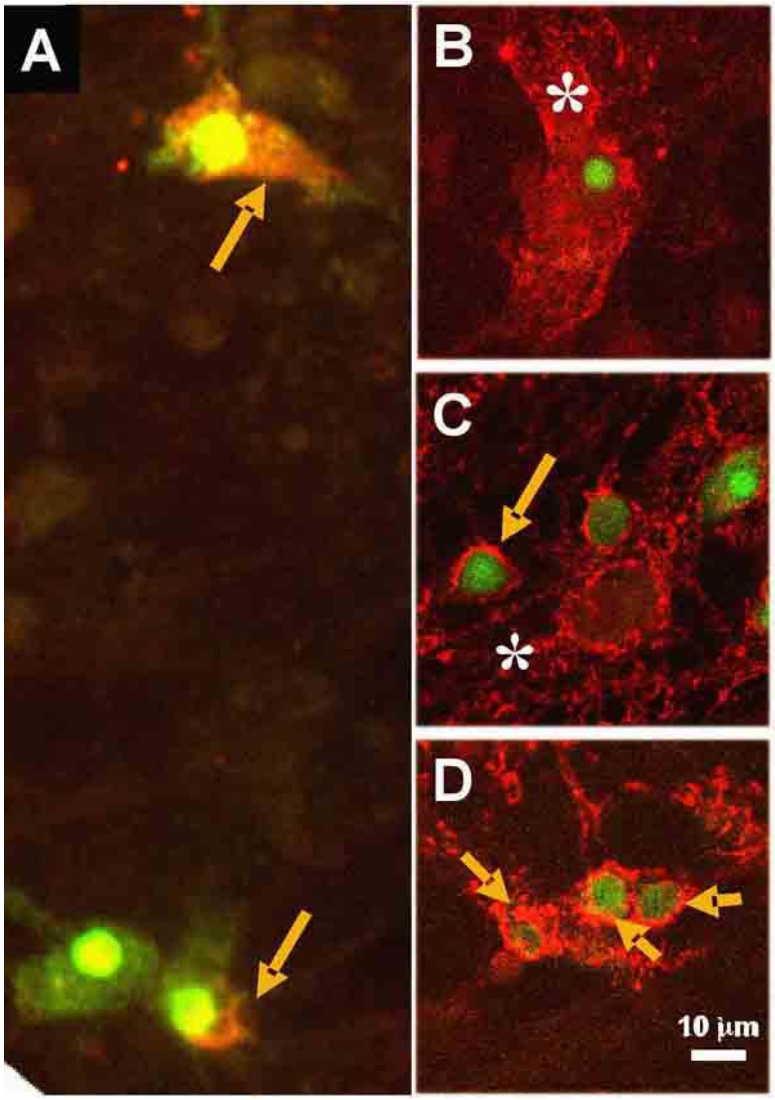

Figure 5. Images of CdSe/CdS-micelles, prepared using modified phospholipids including aPEG, DPPC, and HDA, in cultured rat hippocampal neurons. In this case where aPEG and DPPC are less water soluble, aPEG and DPPC were directly added into QD chloroform solution and water was added after evaporation of chloroform to prepare a QD-micelle aqueous solution. Dispersed cultures of hippocampal neurons, prepared from 3 day old rat pups and grown on polylysine/collegen coated glass coverslips for 2 weeks in Neurobasal A media with B-27 supplement (Invitrogen/GIBCO), were exposed to QD-micelles emitting at 592 nm. After incubation, the cells were fixed in 4% paraformaldehyde/4% sucrose, permeabilized and stained with antibodies to neuronal specific marker NeuN (Chemicon,

Temecula, CA) followed by FITC (Panel A) or Alexa Fluor 488 (Panel B-D) labeled antimouse secondary antibody (Molecular Probes, Eugene OR). Panel A, Fluorescent microscopy image of QD accumulation (red, arrows) after 16 hours of incubation (~ 1mg/ml QD-micelles) in neurons identified by nuclear staining for NeuN (green). Panels B-D, Confocal microscopy of pulse-chase labeling with QD-micelles. Incubation with QD-micelles during depolarization with 55 mM KCl for 10 min (panel B) shows dispersed, punctate staining (indicated by astericks) characteristic of neurite processes; whereas after chase in basal media without QD-micelles for 1 hour (panel C) or 5 hours (panel D) shows increasing perinuclear localization (arrows) with a corresponding decrease in the punctate stain seen in the 10 min labeling. Scale bar, 10 microns, for panels B-D. Images of 1 micron thick optical sections were obtained with a Zeiss Meta System Confocal Microscope using a 40X objective. QDs were imaged using 405 mm excitation and 560-615 nm emission; Alexa 488 NeuN staining with 488 nm excitation and 505-530 nm emission.

appeared to locate to a perinuclear compartment adjacent to NeuN stained neuronal nuclei. The results indicate that under these conditions QDs were effectively taken up by an endocytotic mechanism that was promoted by increased synaptic vesicle recycling and potentially followed by transport to lysosomes. Trafficking of QDs to lysosomal compartments may reflect autophagy, a vesicular-mediated process that underlies catabolic recycling and degradation of macromolecules, including both cellular and xenotypic agents, such as bacteria and viral pathogens. Autophagy may be a particularly critical mechanism for maintaining the cellular integrity of neurons, which are long-lived and generally show little or no turnover in most regions of the nervous system, and could play a role in neuronal cell death under certain conditions. The ability to use QDs to probe the trafficking of autophagic vacuoles promises to provide a useful tool to track this cellular process, but whether this tool itself elicits an autophagic response, precipitating cell death over time, will require further study.

In conclusion, the surfactant/lipid encapsulation method is simple and easy. It can be used to synthesize water-soluble NC-micelles with different shape and compositions. The micelles provide reactive surface chemistry for further conjugation with biospecies, such as

proteins, antibodies, etc., which is essential for their bioapplications. The hydrophilic micelle interface also allows further self-assembly with metal oxides to form ordered NC/metal oxides arrays.

Experimental

1. Synthesis of monodisperse gold nanocrystals[21]: a 60 ml aqueous solution containing 0.7g $HAuCl_4$ (Aldrich) was mixed with a solution of tetraoctylammonium bromide (4g, Aldrich) in 160ml toluene. The two-phase mixture was vigorously stirred until the tetrachloroaurate was transferred completely into the organic layer (judged by color changes: the aqueous phase became colorless and the organic phase became dark yellow). 0.34g dodecanethiol (Aldrich) was added to the organic phase. A 40ml freshly prepared aqueous solution of sodium borohydride (0.78g, Aldrich) was slowly added with vigorously stirring and finished during 20mins. After further stirring for 3hrs, the organic phase was separated and evaporated in a rotary evaporator. Heat treatment at 140˚C was performed for 30 minutes. The gold nanocrystals were then purified by two cycles of precipitation, followed by size-selective precipitation using the solvent/nonsolvent pair of toluene/ethanol.
2. In a general preparation of water soluble gold NC-micelles and 2-, 3-D ordered superlattice, 0.20 g cetyltrimethylammonium bromide ($CH_3(CH_2)_{15}N^+(CH_2)_3Br^-$, Aldrich, or other surfactants) was added to 8-12g DI-water to form solution A. Solution A was sonicated to completely dissolve the surfactant. 0.30 g 1-DT derivatized gold (or other NCs such as Fe_2MnO_4, CdTe, etc) NCs were dissolved in 1-2 ml chloroform to form solution B. Solutions A and B were mixed together with vigorous stirring, and the chloroform was removed by heat treatment to finish the encapsulation. A dark-colored solution (stock solution, C) was finally obtained and centrifuged at 2000rpm for 5mins to remove precipitates if any. Solution C can be further diluted for UV-vis spectroscopy or TEM characterization. 2-D *hcp* superlattice was formed by using diluted stock solution C by adding more water. 3-D superlattice films were prepared by directly drying stock

solution C on glass slides, silicon wafers, and TEM grids. 3-D superlattice films can also be prepared on substrates by spin-coating or casting.

3. The XRD spectra were recorded on a Siemens D500 diffractometer using graphite monochromotor filtered CuKα radiation with λ=1.54Å in θ-2θ (2θ=1-10˚) scan mode using step size ranging from 0.02 to 0.002 and dwell time of 1 to 5. TEM images were taken at JEOL 2010 high-resolution microscope equipped with Gatan slow scan CCD camera and operated at 200 keV.

References

1. Bruchez, M., Moronne, M., Gin, P., Weiss, S. & Alivisatos, A. P. Semiconductor nanocrystals as fluorescent biological labels. Science 281, 2013-16 (1998).
2. Chan, W. C. W. et al. Luminescent quantum dots for multiplexed biological detection and imaging. Current Opinion in Biotechnology 13, 40-46 (2002).
3. Chan, W. C. W. & Nie, S. M. Quantum dot bioconjugates for ultrasensitive nonisotopic detection. Science 281, 2016-18 (1998).
4. Gerion, D. et al. Synthesis and properties of biocompatible water-soluble silica-coated CdSe/ZnS semiconductor quantum dots. Journal of Physical Chemistry B 105, 8861-71 (2001).
5. Larson, D. R. et al. Water-soluble quantum dots for multiphoton fluorescence imaging in vivo. Science 300, 1434-6 (2003).
6. Mattoussi, H. et al. Bioconjugation of highly luminescent colloidal CdSe-ZnS quantum dots with an engineered two-domain recombinant protein. Physica Status Solidi B International Conference on Semiconductor Quantum Dots (QD2000) International Conference on Semiconductor Quantum Dots (QD 2000), 31 July-3 Aug. 2000, Munich, Germany 224, 277-83 (2001).
7. Pellegrino, T. et al. Quantum dot-based cell motility assay. Differentiation 71, 542-548 (2003).
8. Brust, M., Walker, M., Bethell, D., Schiffrin, D. J. & Whyman, R. Synthesis of Thiol-Derivatized Gold Nanoparticles in a 2-Phase Liquid-Liquid System. Journal of the Chemical Society-Chemical Communications, 801-802 (1994).

9. Murray, C. B., Kagan, C. R. & Bawendi, M. G. Self-Organization of Cdse Nanocrystallites into 3-Dimensional Quantum-Dot Superlattices. Science 270, 1335-1338 (1995).
10. Sun, S. H., Murray, C. B., Weller, D., Folks, L. & Moser, A. Monodisperse FePt nanoparticles and ferromagnetic FePt nanocrystal superlattices. Science 287, 1989-1992 (2000).
11. Cao, Y. W. C., Jin, R. C. & Mirkin, C. A. Nanoparticles with Raman spectroscopic fingerprints for DNA and RNA detection. Science 297, 1536 (2002).
12. Dubertret, B. et al. In vivo imaging of quantum dots encapsulated in phospholipid micelles. Science v.298, p.1759-1762 (2002).
13. Mirkin, C. A., Letsinger, R. L., Mucic, R. C. & Storhoff, J. J. A DNA-based method for rationally assembling nanoparticles into macroscopic materials. Nature v.382, p.607-609 (1996).
14. Petruska, M. A., Malko, A. V., Voyles, P. M. & Klimov, V. I. High-performance, quantum-dot nanocomposites for nonlinear-optical and optical-gain. Adv. Mater. 15, 610-613 (2003).
15. Sundar, V. C., Eisler, H. J. & Bawendi, M. G. Room-temperature; tunable gain media from novel II-VI nanocrystal-titania composite matrices. Advanced Materials 14, 739 (2002).
16. Fan, H. Y., Chen, Z., Brinker, C., Clawson, J. & Alam, T. Synthesis of Organo-Silane Functionalized Nanocrystal Micelles and Their Self-Assembly. J. Am. Chem. Soc. 127, 13746-13747 (2005).
17. Fan, H. Y. et al. Ordered Two- and Three-Dimensional Arrays Self-Assembled from Water-Soluble Nanocrystal–Micelles. Adv. Mater. 17, 2587-2590 (2005).
18. Fan, H. Y. et al. Surfactant-assisted synthesis of water-soluble and biocompatible semiconductor quantum dot micelles. Nano Letters 5, 645 (2005).
19. Fan, H. Y. et al. Self-assembly of ordered, robust, three-dimensional gold nanocrystal/silica arrays. Science 304, 567-571 (2004).
20. Shen, L. F., Laibinis, P. E. & Hatton, T. A. Bilayer surfactant stabilized magnetic fluids: Synthesis and interactions at interfaces. Langmuir 15, 447 (1999).

21. Patil, V., Mayya, K. S., Pradhan, S. D. & Sastry, M. Evidence for novel interdigitated bilayer formation of fatty acids during three-dimensional self-assembly on silver colloidal particles. Journal of the American Chemical Society 119, 9281 (1997).
22. Nikoobakht, B. & El-Sayed, M. A. Evidence for bilayer assembly of cationic surfactants on the surface of gold nanorods. Langmuir 17, 6368 (2001).
23. Peng, X. G. et al. Shape control of CdSe nanocrystals. Nature 404, 59-61 (2000).

Distribution

2	MS1349	Hongyou Fan, 1815-1
1	MS1349	C. Jeffrey Brinker, 1002
4	MS1349	Carol S. Ashley, 1815-1
1	MS1411	David Tallant, 1822
2	MS9018	Central Technical Files, 8945-1
2	MS0899	Technical Library, 9616
1	MS0161	Patent and Licensing, 11500
1	MS0123	LDRD Program Office, 01011


Sandia National Laboratories